



Chemosensory function of *Varroa gnathosoma*: transcriptomic and proteomic analyses

Beatrice T. Nganso^{1,2} · Nurit Eliash^{3,4,5} · Kannan Mani¹ · Noa Sela⁶ · Alejandro Villar-Briones⁷ · Angelina Fathia Osabutey¹ · Ada Rafaeli⁸ · Alexander S. Mikheyev^{3,9} · Victoria Soroker¹

Received: 17 October 2023 / Accepted: 18 July 2024 / Published online: 23 October 2024
© The Author(s) 2024

Abstract

In this study, we evaluated the role of the gnathosoma (mouthparts) in chemosensing of the most devastating honey bee parasite, *Varroa destructor* mite. Through transcriptomic analysis, we compared the expression of putative chemosensory genes between the body parts containing the main chemosensory organs (the forelegs), gnathosoma and the rest of the body devoid of these two body parts. Furthermore, we checked the presence of chemosensory-related transcripts in the proteome of the gnathosoma. Our comparative transcriptomic analysis revealed the presence of 83 transcripts with known characteristic conserved domains belonging to eight chemosensory gene families in the three *Varroa* transcriptomes. Among these transcripts, 11 were significantly upregulated in the mite's forelegs, compared to 8 and 10 in the gnathosoma and body devoid of both organs, respectively. Whilst the gnathosoma and the forelegs share similar expression of some putative lipid carrier proteins, membrane-bound receptors, and associated proteins, they also differ in the expression profiles of some transcripts belonging to these protein families. This suggests two functional chemosensory organs that may differ in their chemosensory function according to specific characteristics of compounds they detect. Moreover, the higher expression of some chemosensory transcripts in the body devoid of forelegs and gnathosoma compared to the gnathosoma alone, may suggest the presence of additional function of these transcripts or alternatively presence of additional external or internal chemosensory organs. Insights into the functional annotation of a highly expressed gustatory receptor present in both organs using RNA interference (RNAi) are also revealed.

Keywords Sensory organs · Lipid carrier proteins · Membrane-bound receptors and proteins · Honey bee parasitic mite

Introduction

Olfaction, as well as gustation, are essential for animal survival and fitness, allowing behavioral modulation according to environmental input thus optimizing the detection of food, mates, and enemy-avoidance *via* volatile and contact chemicals. However, the molecular structure and function of the chemosensing organs are not well known in non-insect arthropods in general, and Acari (mites and ticks) in particular. As a model organism, we are studying the obligatory ecto-parasitic mite, *Varroa destructor* (Anderson and Trueman) (Parasitiformes, Mesostigmata, Varroidae), considered as the major pest of the Western honey bee almost worldwide (Traynor et al. 2020). The life cycle of the *Varroa* mite is tightly synchronized with the development of the honey bee and the health status of the colony. It consists of two main phases: a reproductive and a non-reproductive (i.e., dispersal) phase (Martin 2001; Rosenkranz et al. 2010). During the dispersal phase, the female mite usually parasitizes an adult bee either nurse or forager and spreads within or between the colonies. During the reproductive phase, the female mite parasitizes the cell containing a fifth instar honey bee larva and reproduces within the cell till the emergence of the adult bee (Martin 2001). Detection of the honey bee stage and colony condition occurs via the mite's eavesdropping on host honey bee chemical cues (Frey et al. 2013; Nazzi and Le Conte 2016; Pernal et al. 2005; Plettner et al. 2017). Information on *Varroa*'s host searching and selection behavior and the nature of chemical cues from the host bee and their environment that regulate its reproduction suggests that both high (e.g. geraniol, 8-heptadecene, nerolic acid) and low (fatty acid methyl and ethyl esters, hydrocarbons C21-C29) volatile molecules are perceived by the mite (Nazzi and Le Conte 2016; Plettner et al. 2017; Soroker et al. 2019).

The occurrence of a few chemosensory organs might be adaptive to ensure the survival of most if not all studied terrestrial arthropods. It enables not only to create a broader chemical picture by receiving a wide range of environmental cues but also a backup, to maintain chemosensory abilities in case of a failure in one of the organs. In the case of the honey bee parasitic *Varroa* mite, two sites with putative chemosensory sensilla are the forelegs and the gnathosoma (Dillier et al. 2006). The fact that while walking *Varroa* holds their forelegs above the ground in a similar manner to antennae in other arthropods points towards the role of the forelegs in volatile detection. The presence of nine chemosensory sensilla located inside a pit and 9 more sensilla surrounding it on the distal dorsal part of each foreleg, analogous to Haller's organ found in ticks, further indicated foreleg function in *Varroa* host chemosensing (Dillier et al. 2006). Liu and Peng (1990) reported that some of the *Varroa* pedipalpi setae are tip pore sensilla and thus could play a potential role in its host chemosensing, but (Dillier et al. 2006), did not indicate any chemosensory sensilla in the pedipalpi and stated that their four segments are covered by strong trichoid setae and in addition, each distal segment of the pedipalpi contains long setae.

Focusing on the role of host sensing by *Varroa* forelegs, we showed their clear ability to sense both nurse and forager honey bee volatiles as well as the honey bee pheromone, E- β -ocimene (Eliash et al. 2014; Singh et al. 2015). Moreover, we showed that disruption of foreleg volatile chemosensing by specific dialcoxybenzenes, cyclopentenol ethers and N, N-Diethyl-m-toulamide (DEET) is reflected in changes in host preference and detection abilities by free moving mites (Eliash et al. 2014; Singh et al. 2015). On the other hand, our recent study demonstrated that host recognition ability in foreleg varnished mites dropped to about 40% within the first hour of the bioassay relative to about 80% of foreleg-unvarnished

mites (Nganso et al. 2020). Additionally, only about 20% of mites remained on the host three hours following mechanical blocking of the main olfactory organ on the forelegs and only one mite was feeding relative to about 80% and 35% of foreleg-unvarnished mites, who remained and fed on the host, respectively. Overall, these findings suggested that the sensilla of the gnathosoma have relatively minor chemosensory function when compared to those of the forelegs.

Focusing on the forelegs as the main chemosensory organ and based on assumption of general similarity in the chemosensory mechanisms in arthropods, we and other colleagues analyzed transcriptome of *Varroa* forelegs. We have not found chemosensory proteins (CSPs) and odorant receptors (ORs) but identified some chemosensory-related gene transcripts. These belong to eight protein families, some are conserved across Arthropoda but others are arachnid-specific (Eliash et al. 2017, 2019; Iovinella et al. 2018; Zhu et al. 2021a, b). These include transcripts of soluble odorant carrier proteins as well membrane associated proteins and receptors. Among carrier proteins, transcripts of the members of three groups were identified: Niemann-Pick type C2 (NPC2) protein, odorant binding proteins (OBPs) and lipocalins, while among membrane-bound receptors and associated proteins, members of six groups were detected: ionotropic glutamate receptors (IGRs), ionotropic receptors (IRs), gustatory receptors (GRs), sensory neuron membrane proteins (SNMPs), transient receptor potential proteins (TRPs) and epithelial Na⁺ channel (ENaCs) proteins. Among these chemosensory gene families, some were found to be significantly up-regulated in the forelegs compared to the other legs; thereby implicating their putative role in *Varroa* host chemosensing (Eliash et al. 2019). On the other hand, proteomic analyses of *Varroa* forelegs only detected proteins belonging to the OBP, NPC2, IGR and SNMP families (Eliash et al. 2019; Iovinella et al. 2018), with few OBP and NPC2 proteins significantly upregulated in this chemosensory organ (Eliash et al. 2019).

Recently, we demonstrated via RNA interference that silencing two NPC2 transcripts evoke different physiological effects on the mites. Silencing one highly expressed and foreleg-specific NPC2 transcript (*LOC111247660*), referred to as *Vd40090* in (Eliash et al. 2017), reduced feeding and reproduction of the mite without affecting host reaching ability, suggesting its involvement in the detection of short-range host cues (Nganso et al. 2021). In contrast, silencing the other NPC2 transcript (*LOC111247342*) referred to as *Vd74517* in (Eliash et al. 2017) significantly disrupted only the host reaching ability, thus indicating the crucial role of this putative odorant carrier protein in the detection of long-range host cues (Mani et al. 2022). Additionally, recently via an exclusion of the chemosensory appendages (forelegs, gnathosoma or both), we showed that in the absence of the forelegs, the expression level of at least one of the putative odorant binding proteins belonging to the NPC2 family previously reported in the forelegs (Eliash et al. 2019) are expressed in the gnathosoma (Nganso et al. 2021).

Whilst we know the identity of some putative chemosensory-related transcripts in *Varroa*'s forelegs (Eliash et al. 2019, 2017; Iovinella et al. 2018), and the role of a few of them in *Varroa*-host interaction (Nganso et al. 2021; Mani et al. 2022), the identity of those associated with gnathosoma and their functional significance are not well understood. So far, it is only the presence of lipid carrier proteins belonging to the OBP and NPC2 families that was reported in *Varroa* mouthparts via proteomic analysis (Iovinella et al. 2018). Therefore, our aim in this study was to compare the expression profile of putative chemosensory genes

between the two chemosensory organs and to functionally annotate one highly expressed gustatory receptor present in both organs using RNA interference (RNAi).

Materials and methods

Collection of mites

Experimental honey bee colonies of *Apis mellifera ligustica* maintained in Langstroth hives at the Agricultural Research Organization, Volcani Center, Israel were used in the course of this study. These experimental colonies were not treated against *V. destructor* and received 60% sugar solution and 70% pollen cake seasonally when needed. The mites were collected from honey bees in these colonies by the sugar shake method (Dietemann et al. 2013). The mites were kept on moist filter paper and dissected within an hour following collection.

Transcriptomics

Total RNA extraction

Within an hour of mite collection, an individual mite was put immediately into a 1.5 ml Eppendorf tube dipped in liquid nitrogen or was first dissected using a fine surgical blade (size no. 11) under a stereo microscope (Olympus SZX12, Shinjuku-ku, Tokyo, Japan). Three groups of samples were collected: (1) gnathosoma only, (2) mites without both the gnathosoma and forelegs (WB_minus), and (3) mites with both the gnathosoma and forelegs (WB_plus). Each treatment group contained a pool of approximately 300 individuals in four replicates (in total 1200 mites per treatment group). The samples were subsequently kept at $-80\text{ }^{\circ}\text{C}$ until total RNA extraction. Total RNA was extracted from each replicate as described before by Nganso et al. (2021). In short, samples in the 1.5 ml Eppendorf tubes were dipped in liquid nitrogen, ground and extracted for total RNA using a Geneall Kit (Geneall, Seoul, South Korea) following the manufacturer's protocol. Elimination of genomic DNA contamination from the RNA samples was done using the TURBO DNA-free™ Kit (Thermo Fisher Scientific, Lithuania, USA) according to the manufacturer's instructions. The samples were eluted from the column with 25 μl of RNase-free water supplied within the GeneAll kit before checking the quality and quantity of the RNA samples on a NanoDrop 2000 spectrophotometer (Thermo Scientific, Wilmington, DE, USA). The RNA samples were subsequently kept at $-80\text{ }^{\circ}\text{C}$ until shipment in dry ice to the Okinawa Institute of Science and Technology (OIST) in Japan for transcriptomic analysis.

RNA library preparation and sequencing

RNA quality and quantity were measured by NanoDrop spectrophotometer (Thermo Fisher Scientific, Japan), and Bioanalyzer 2100 with RNA Pico kits (Agilent, Japan). Libraries were prepared using Nextera XT Prep kit (Illumina, Japan) as described before (Aird et al. 2013). In brief, 200 ng of total RNA were used to prepare cDNA libraries, amplified in 16 PCR cycles, and purified using 16% PEG SPRI. The cDNA concentration was measured using Qubit fluorometer (Thermo Fisher Scientific, Japan), and quality checked using 4200

TapeStation with a high-sensitivity D5000 kit (Agilent, Japan). For sequencing, 0.2 ng of amplified cDNA were used in two lanes of Illumina HiSeq 2500 at the OIST sequencing center in 250 paired-end mode, according to manufacturer's specifications.

Mapping, transcriptome analysis and chemosensory-related gene annotations

The raw read sequences from the three RNA samples were uploaded to the National Centre for Biotechnology Information (BioProject accession PRJNA872955). The reads were cleaned to remove adaptor sequences and reads with low quality scores using Trimmomatic software (Bolger et al. 2014). Cleaned reads were mapped to the reference genome of *Varroa* mite (GCF_002443255.1) (Techer et al. 2019) using Tophat 2 with the default parameters (Kim et al. 2013). Additionally, the former clean reads extracted and sequenced previously from the forelegs and rear legs of *Varroa* mite generated by (Eliash et al. 2019) were also mapped to the reference genome of the mite. Quantification and de-novo analysis of the new transcript was done using cufflinks, cuffquant and cuffnorm software package suit (Trapnell et al. 2012). Subsequently, the principal component analysis (PCA) was calculated among the three groups: gnathosoma, WB_minus and WB_plus using the function pcomp in R. Counts were normalized and P-values and log₂fold change (the rate of change between the two values after logarithmic transformation) were computed by the DESeq package (Anders et al. 2010). Based on the multiple hypothesis correction (Benjamini and Hochberg 1995), P-values were adjusted (padj). The threshold for significant differential gene expression was set at padj ≤ 0.05 and log₂ fold change ≥ 1. The Venn diagram was also constructed using the tool Venny version 2.1.0 (Oliveros 2007–2015) to show the distribution of differentially expressed genes among the three RNA groups. Following transcriptomic analysis, a protein database was constructed from the transcriptome assembly of the gnathosoma only to be used for proteomics analysis. Each oriented and un-oriented transcript was translated into amino acids using Transdecoder software (Haas, n.d.). In order to search for orthologues of all the assembled contigs belonging to OBP, NPC2, CSPs, ORs, IGRs, IRs, GRs, SNMPs, TRPs and ENaCs chemosensory-related families previously searched in *Varroa*'s forelegs and rear legs (Eliash et al. 2017, 2019), BLASTx was used along InterProScan (Quevillon et al. 2005) to identify the conserved domains specific to each transcript group as described before (Eliash et al. 2017, 2019). We also searched for transcripts of the nine lipocalins found in the genome of *V. destructor* (XP_022658018, XP_022661284, XP_022665322, XP_022671613, XP_022662731, XP_022653636, XP_022653633, XP_022664566, XP_022663986) (Zhu et al. 2021b) in the transcriptomes of the three RNA groups of this study and those of *Varroa*'s forelegs and rear legs (Eliash et al. 2019).

Proteomics

Protein extraction

All chemicals were purchased from Sigma Aldrich (St Louis MO, USA). Proteins were extracted from *Varroa* gnathosoma samples only (a pool of at least 300 individuals, in four replicates as described above). Samples were manually crushed after adding 400 µl of SDT lysis buffer (0.1 M Tris pH 7.6, 0.1 M dithiothreitol, 4% sodium dodecyl sulfate) and placed in 4 °C overnight before subjecting to heating at 95 °C for 10 min followed by cooling for

5 min. at room temperature. Protein quantification in each sample with Bradford method (Bio-Rad Protein Assay) was done before shipping the samples in dry ice to OIST in Japan for proteomic analysis.

Protein digestion and purification

We used the S-Trap method for protein preparation. First, the crude protein extracts were sonicated (QSONICA Q800R, Thermo Fisher Scientific), heated at 60 °C for 30 min and alkylated by incubating in iodoacetamide (Wako, Japan) for 30 min in darkness. After centrifugation, the supernatant was used for S-Trap digestion following the procedure described by (HaileMariam et al. 2018). In brief, protein concentration was measured using MilliQ Direct Detect IR spectrometer (Merck, Japan), and 50 µg of each sample were acidified with phosphoric acid (Wako, Japan). After adding triethylammonium bicarbonate (Sigma, Japan) in methanol buffer (Thermo Optima, Japan), the samples were passed through a S-Trap tip, and digested with Trypsin (Promega, USA) at 37 °C overnight. The samples were then washed with 0.1% formic acid in water solution (Thermo, Japan), followed by 0.1% formic acid in 60% acetonitrile (Wako, Japan), vacuum dried, resuspend with 1% acetic acid, 0.5% formic acid and sonicated for 5 min. The proteins were then purified following the StageTip protocol (Rappsilber et al. 2007), vacuum dried and resuspended in 1% acetic acid, 0.5% formic acid prior to liquid chromatography and mass spectrometry (LC/MS) analysis.

Liquid chromatography and mass spectrometry

LC/MS was carried out using an ACQUITY M-Class UPLC (Waters corporations) connected to Orbitrap Fusion Lumos mass spectrometer (Thermo Fisher). Five µl of sample were loaded in 0.1% formic acid in acetonitrile (solvent B) onto a trap column (nanoACQUITY UPLC 2G-V/M Trap 5 µm Symmetry C18, 180 µm x 20 mm, Waters). Peptides were separated on the analytical column (nanoACQUITY UPLC HSS T3 1.8 µm, 75 µm x 150 mm, Waters) at 40 °C at a flow rate of 500 nanoLiter/min using a gradient starting from 10% B (initial conditions) followed by 10% B (0–8 min), 95% B (8–8.3 min) and 10% B (8.3–14 min). The mass spectrometer was operated in positive ion mode at a spray voltage of 2.4 kV, in duration of 120 min, resolution of 120,000, scan range of 400–1,500 m/z, AGC target of 4e5 with a maximum injection time of 50 msec. The internal mass calibration was 445.12003 m/z, and the time between master scans lasted for 3 s. We applied the following filters: include charge states to 2–7, dynamic exclusion after 1 time, 12 s, exclude isotopes and the intensity set to higher than 5.0e4. in the data dependent scan, we set the isolation window to 1.2 m/z, collision energy mode was fixed, HCD Collision Energy was 25%, detector resolution set to 15,000, maximum injection time set to 40 msec, and the data type is Centroid.

Proteomic data processing and analysis

Proteome Discoverer software (Thermo Fisher scientific, version 2.2), was used to search against combined databases including: cRAP (for contaminants), predicted proteins in gnathosoma based on the current transcriptome study and predicted proteins based on *Varroa* whole genome sequencing (<https://www.ncbi.nlm.nih.gov/protein/?term=varroa+destruc>)

tor). The minimum and maximum precursor masses were set to 350 and 5,000 Da respectively, total intensity threshold set to 100, and the minimum pick count as 5. A maximum of two trypsin mis-cleavages were allowed with a precursor mass tolerance of 20 ppm, fragment mass tolerance of 0.7 Da, maximum peptide length of 144 and minimum of 7 amino acids. Carbamidomethyl+57.021 Da (C) was selected as static modification, and deamidated+0.984 Da (N, Q) and oxidation+15.994915 (M, P) as dynamic modifications. We set the false discovery rate (FDR) to 0.01 for protein and peptide levels, and the data was normalized to the total protein abundance. The mass spectrometry proteomics data have been deposited to the ProteomeXchange Consortium (<http://proteomecentral.proteomexchange.org>) via the PRIDE partner repository (Perez-Riverol et al. 2022), with the dataset identifier PXD053065.

Silencing of target GR transcript (LOC111245174)

We designed two sets of primers from two different sources for silencing the target GR transcript (Supplementary Table S1). To determine the amplification efficiency of these pairs of primers, the total RNA was extracted from a pool of five mites in eight biological replicates using the GeneAll Kit (Seoul, South Korea) following the manufacturer's protocol. The concentration and quality of each RNA sample was then checked using a NanoDrop 2000 spectrophotometer (Thermo Scientific, Wilmington, DE, USA). Single-strand cDNA (20 ng/ μ L) was generated with the RNA samples (0.4 μ g) using the qPCRBIO cDNA Synthesis Kit (Thermo Scientific, Waltham, MA, USA) following the manufacturer's instructions. Subsequently, these cDNA samples were used to verify the amplification efficiencies of each set of primers using both PCR and RT-qPCR as in Nganso et al. (2021). Following successful amplification, the silencing primers with T7 promoters were purchased and used for *LOC111245174*-dsRNA syntheses as described in detail by Nganso et al. (2021).

The silencing of the target transcript was performed by a non-invasive method of dsRNA delivery to *Varroa* mites as in Nganso et al. (2021). A total of 60 adult mites were soaked in 50 μ L of *LOC111245174*- dsRNA (2.5–4 μ g/ μ l) in 10% NaCl (saline) solution in five biological replicates of 12 mites each. The control mites were soaked in 10% saline solution in eight biological replicates of 12 mites each. To test for silencing of *LOC111245174* transcript, total RNA was extracted from pools of mites that had recovered 15 h after soaking as described above. The cDNA synthesized from the RNA sampled were used for RT-qPCR using a second set of primers that did not overlap with the pairs of primers used for *LOC111245174*-dsRNA syntheses (Supplementary Table S1). The relative expression level of target transcript in each treatment category was calculated after normalization with 18 S rRNA using the $2^{-\Delta\Delta CT}$ approach.

Statistical analysis of proteomic data

For the proteomics analysis, the results from Proteome Discoverer were imported to Perseus software version 1.6.14.0 (<https://maxquant.net/perseus/>), and the abundance data was filtered for contaminants and missing values. Log₂ transformed data was used to produce a volcano plot using a two-sided t-test, with 250 randomizations, FDR=0.05 and $s_0=1$. A one-way ANOVA followed by a post hoc Tukey–Kramer test was used to compare the expression levels of the *LOC111245174* transcripts among the three treatment groups (mites

soaked in saline, 2.5–4 $\mu\text{g}/\mu\text{l}$ LOC111245174-dsRNA) in JMP[®], 14, SAS Institute Inc., Cary, NC, 1989–2019.

Results

Transcriptomics and differential gene expression analysis

Twelve RNAseq libraries of three types of *Varroa* tissues (with four replicates each): gnathosoma (Fig. 1A), whole body without gnathosoma (WB_minus), and whole body (WB_plus), were mapped to *V. destructor* genome (Techer et al. 2019). Principal component analysis was calculated based on a normalized count table. The PCA shows that the gene expression profiles of gnathosoma clearly differs from the other two groups: the WB_minus and the WB_plus (Fig. 1B and Supplementary Fig. S1). Of the 2,067 differentially expressed genes, 1,855 (89.74%) differ between WB_plus and gnathosoma and 961 (46.49%) differ between WB_minus and gnathosoma. In contrast, the gene expression profile of the WB_minus and WB_plus groups seems to be highly similar (Fig. 1B and Supplementary Fig. S1). In fact, only 13 (0.63%) of the 2,067 differentially expressed genes differ between both groups of tissues (Fig. 1C and Supplementary Table S2). Among these 13 genes, one (LOC111246989) was a chemosensory transcript belonging to the OBP-like group (Supplementary Table S2). It was found to be highly expressed in the WB_plus compared to the WB_minus and in both forelegs and gnathosoma and was even detected in gnathosoma proteome (Fig. 2).

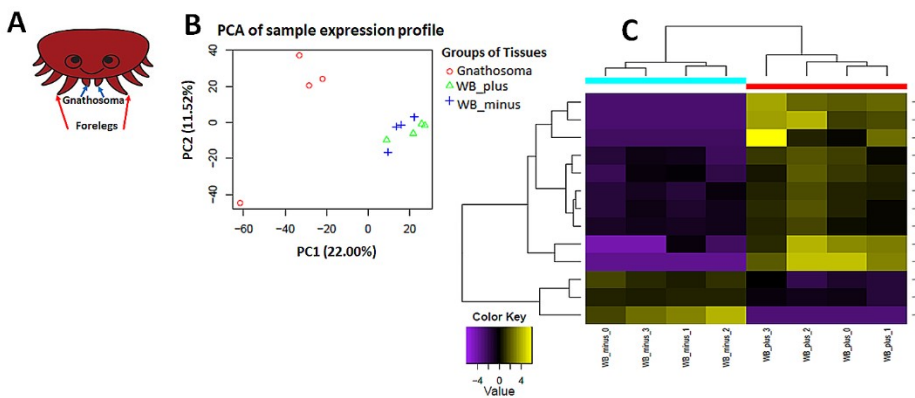


Fig. 1 Transcriptome of differential gene expression for the three RNAs groups: gnathosoma only (gnathosoma), mites without gnathosoma and forelegs (WB_minus), and mites with both the gnathosoma and forelegs (WB_plus). **(A)** A schematic diagram of a *Varroa* mite, dorsal view: marked with red arrows is the pair of forelegs and marked with blue are the gnathosoma. **(B)** Principal components analysis (PCA) of gene expression separated the samples by their groups. The values used for the analysis are based on the 2067 differentially expressed genes with threshold of $\text{FDR} < 0.05$ and $\log_2\text{FC}$ greater than one or lower than minus one. **(C)** Heat map of the 13 differentially expressed genes between the WB_minus and WB_plus. \log_2 of the normalized reads are displayed as the color scale with downregulated genes in purple and upregulated genes in yellow

Locus ID	Transcript ID (Eliash et al 2019)	Transcript ID (this study)	Comparison Groups	A Transcriptome			B Proteome
				WB_plus WB_minus	Gnathosoma WB_minus	Forelegs Rear legs	Gnathosoms
LOC111252778	TRINITY_DN24516_c0_g2_i1	XP_022666940.1	Insect OBPs = 5	-1.06	1.17*	-0.31	-
LOC111247116	TRINITY_DN30972_c0_g1_i2	XP_022653427.1		-0.77	1.10	3.86*	-
LOC111255154	TRINITY_DN23985_c0_g1_i1	XP_022672551.1		0.73	-0.84	0.24	✓
LOC111243821	TRINITY_DN97899_c0_g2_i1	XP_022645714.1		0.10	-1.50***	-0.23	✓
LOC111255133	Not found	XP_022672530.1		-	0.49**	0.34	✓
LOC111246989	TRINITY_DN21610_c0_g1_i1	XP_022653252.1	OBP-like = 2	1.16***	2.85***	2.49***	✓
LOC111247024	TRINITY_DN81792_c0_g1_i1	XP_022653281.1		0.21	-0.77**	-0.20	✓
LOC111247660	TRINITY_DN21033_c0_g2_i1	XP_022654596.1	NPC2 = 4	4.32***	4.64	10.99***	-
LOC111245340	TRINITY_DN66140_c0_g1_i1	XP_022649311.1		0.02	-0.09	0.13	✓
LOC111246599	TRINITY_DN80297_c0_g1_i1	XP_022652195.1		0.53	-0.55	-1.20	-
LOC111247342	TRINITY_DN99150_c0_g1_i1	XP_022653875.1		0.03	-1.11	0.81	-
LOC111249022	TRINITY_DN67339_c0_g1_i1	XP_022658018	Lipocalins = 6	-0.5	-0.6*	-2.44	✓
LOC111250379	TRINITY_DN21422_c0_g1_i1	XP_022661284		0.34	-1.83***	-1.99**	-
LOC111252121	TRINITY_DN19228_c0_g1_i1	XP_022665322		0.05	0.28	-0.13	✓
LOC111247224	TRINITY_DN21300_c0_g1_i1	XP_022653636		2.45*	3.03	5.24*	-
LOC111251803	TRINITY_DN25264_c0_g1_i1	XP_022664566		0.73	-0.18	12.19***	-
LOC111251576	TRINITY_DN89651_c0_g1_i1	XP_022663986		1.69	0.94	8.93***	-
LOC111247324	TRINITY_DN27769_c0_g1_i3	XP_022653836.1	IGRs = 25	-0.25	0.96#	-0.53	✓
LOC111246329	TRINITY_DN29108_c0_g3_i3	XP_022651534.1		0.38	-0.85	0.01	-
LOC111244349	TRINITY_DN29235_c0_g3_i1	XP_022647089.1		0.64	0.94	-0.14	-
LOC111255360	TRINITY_DN30590_c1_g1_i1	XP_022672996.1		0.00	0.00	0.53	-
LOC111247344	TRINITY_DN31016_c0_g1_i1	XP_022653881.1		0.56	0.32	0.34	-
LOC111248023	TRINITY_DN31641_c0_g1_i1	XP_022655446.1		-0.76	0.36	-0.39	✓
LOC111246347	TRINITY_DN6650_c0_g2_i1	XP_022651543.1		-0.67	0.78	-1.18	✓
LOC111246476	TRINITY_DN29652_c0_g2_i1	XP_022651879.1		0.80	1.07	-0.06	-
LOC111251000	TRINITY_DN30559_c1_g1_i3	XP_022663473.1		-1.02	0.79	-0.23	-
LOC111244732	NF	XP_022647828.1		-0.22	0.50	0.15	-
LOC111243331	NF	XP_022644440.1		0.99	-1.30	-0.60	✓
LOC111248674	NF	XP_022657179.1		-0.61*	0.43*	-0.59	✓
LOC111247991	NF	XP_022655389.1		-0.23	0.63	-0.12	-
LOC111251125	NF	XP_022663165.1		0.08	-3.24	0.95	-
LOC111252394	NF	XP_022665938.1		-0.49	0.75	0.74	-
LOC111243762	NF	XP_022645545.1		-2.03	2.64	0.21	-
LOC111250771	NF	XP_022662237.1		-0.04	-1.41	0.54	-
LOC111247409	NF	XP_022654019.1		-0.08	-0.90	0.40	-
LOC111246056	NF	XP_022651004.1		-0.21	-0.86	-0.44	-
LOC111246314	NF	XP_022651423.1		-0.32	0.82	0.37	-
LOC111245193	NF	XP_022648928.1		2.35*	0.67	0.53	-
LOC111244237	NF	XP_022646826.1		2.23*	-0.52	1.59	-
LOC111248359	NF	XP_022656295.1		0.77	-0.04	0.13	-
LOC111250813	NF	XP_022662330.1		0.31	-4.90	1.48	-
LOC111255164	NF	XP_022672562.1		2.58	0.58	-0.80	-
LOC111251297	TRINITY_DN25813_c0_g1	XP_022663474.1	IR25a = 1	0.25	1.16	5.99***	-
LOC111245174	TRINITY_DN23243_c0_g1_i2	XP_022648881.1		3.86	6.57***	4.50*	-
LOC111254617	TRINITY_DN26187_c0_g2_i1	XP_022671394.1	GRs = 2	-0.76	-0.69	0.87#	✓
LOC111246589	TRINITY_DN24266_c1_g1_i1	XP_022652187.1		-0.38	-0.23	0.03	✓
LOC111247539	TRINITY_DN24854_c0_g1_i1	XP_022654312.1	-0.54	0.41	-0.27	✓	
LOC111255378	TRINITY_DN26930_c0_g1_i11	XP_022673028.1	SNMPs = 5	0.78	-1.53**	-1.03	-
LOC111245055	NF	XP_022648629.1		0.51	-0.68	0.28	-
LOC111255252	NF	XP_022672748.1		0.29	-0.36	0.13	-
LOC111243805	TRINITY_DN30598_c0_g1_i2	XP_022645664.1		1.61	2.54*	0.62	-
LOC111245614	TRINITY_DN30964_c0_g1_i1	XP_022650015.1		-0.29	0.52	0.19	-
LOC111251668	NF	XP_022664221.1	0.31	-1.12*	-0.14	✓	
LOC111243271	NF	XP_022644287.1	-0.36	-0.99*	0.11	-	
LOC111248665	NF	XP_022657121.1	-1.09*	1.18*	-0.36	-	
LOC111244142	NF	XP_022646609.1	0.37	1.80	1.75	-	
LOC111247160	NF	XP_022653516.1	-0.34	-1.62	-1.40	-	
LOC111248369	NF	XP_022656312.1	-1.82	-2.08	-0.58	-	
LOC111248272	NF	XP_022656071.1	-0.58	0.92	-0.77	-	
LOC111243445	NF	XP_022644771.1	-0.19	0.24	-0.77	✓	
LOC111251363	NF	XP_022663608.1	0.06	0.20	-0.18	-	
LOC111253616	NF	XP_022669032.1	-0.53	0.60	-0.05	-	
LOC111250995	NF	XP_022662844.1	-0.75	-0.28	-0.15	-	
LOC111253656	NF	XP_022669108.1	0.13	0.08	0.05	-	
LOC111245815	NF	XP_022659388.1	0.44	-0.47	0.45	-	
LOC111254129	NF	XP_022670412.1	0.73	0.09	0.44	-	
LOC111253116	NF	XP_022667812.1	-1.27#	-0.11	0.08	-	
LOC111252233	NF	XP_022672722.1	0.77	0.09	0.09	-	
LOC111254284	NF	XP_022670699.1	1.27	0.00	-0.65	-	
LOC111253486	NF	XP_022668666.1	0.47	-0.74	-0.06	✓	
LOC111248411	NF	XP_022656458.1	0.04	1.08	1.24	-	
LOC111246367	TRINITY_DN26906_c0_g1_i1	XP_022651586.1	ENaCs = 12	-1.48	-0.05	-0.15	-
LOC111254848	TRINITY_DN29020_c0_g2_i2	XP_022671866.1		-0.50	-3.91	2.51***	-
LOC111245781	TRINITY_DN29690_c0_g2_i4	XP_022650281.1		-0.82	0.95	1.29	-
LOC111244963	TRINITY_DN29889_c0_g1_i2	XP_022648331.1		2.52	0.00	3.19***	-
LOC111251329	TRINITY_DN30734_c0_g1_i6	XP_022663539.1		0.00	4.54	5.23***	-
LOC111250651	TRINITY_DN65984_c0_g1_i1	XP_022661917.1		0.65	-1.02	-0.25	-
LOC111248172	NF	XP_022655765.1		0.75	0.14	3.25	-
LOC111249780	NF	XP_022665280.1		2.03	2.97	0.22	-
LOC111251743	NF	XP_022664406.1		-0.07	0.41	0.25	-
LOC111247984	NF	XP_022655370.1		1.24	1.02	0.14	-
LOC111253877	NF	XP_022669766.1		-0.68	-2.68*	2.47	-
LOC111246582	NF	XP_022652151.1		0.15	-0.31	0.87	✓



Fig. 2 (A) Heat map of the chemosensory related differentially expressed gene transcripts. 83 transcripts identified in eight chemosensory groups, in three RNAs comparisons: gnathosoma, mites without gnathosoma and forelegs (WB_minus), and mites with both the gnathosoma and forelegs (WB_plus). Log2 fold change of the normalized reads are displayed at the bottom of the heat map, in colour scale (highest value=15, lowest value=-2). Black asterisks “*”, “**”, “***”, “****” indicate significantly upregulated genes in the different comparisons (log2 fold change ≥ 1 ; Padj $\leq 0.05, 0.001, 0.0001$); “#” indicates those that were close to significance (log2 fold change ≥ 1 ; Padj = 0.05; and “NF” indicate new transcripts detected in this study that was not previously reported by (Eliash et al. 2019) in the transcriptomes of the forelegs and rear legs of *Varroa*. Purple asterisks “*”, “**”, “***”, “****” indicate significantly downregulated genes in the different comparisons (log2 fold change ≤ -1 ; Padj $\leq 0.05, 0.001, 0.0001$). (B) Twenty-one proteins identified in the proteome of the gnathosoma. Average intensity ratios are displayed at the bottom of the heat map, in colour scale (highest value=70, lowest value=0). OBPs (odorant-binding proteins); NPC2 (Niemann-Pick type C2 protein); IGRs (ionotropic glutamate receptors); IRs (ionotropic receptors); GRs (gustatory receptors); SNMPs (sensory neuron membrane proteins); TRPs (transient receptor potential proteins); ENaCs (degenerin/epithelial Na⁺ channel proteins)

Annotation and differential gene expression analysis of chemosensory-related transcripts and proteins

In the current study, we found 83 transcripts belonging to OBP, NPC2, lipocalins, IGR, IR, GR, SNMP, TRP and ENaCs chemosensory-related families in the three transcriptome libraries studied herein: gnathosoma, WB_plus and WB_minus (Table 1, and Fig. 2). No odorant receptor or chemosensory protein were found. The re-mapping of *Varroa* foreleg and rear legs transcriptomes generated by Eliash et al. (2019) to the reference genome of the mite also revealed the presence of all these 83 transcripts (Table 1; Fig. 2). These transcripts were classified into their respective families based on the presence of their conserved characteristic domains and GO terms (see Table 1 in (Eliash et al. 2017) and Table 2 in (Eliash et al. 2019). The identified chemosensory related transcripts included both lipid carrier proteins (17 transcripts), presumably carrying and solubilizing odors, and membrane-bound proteins, hypothetically acting as chemoreceptors or co-receptors (66 transcripts). Of the carrier proteins, seven belong to the OBP (five were insect OBP transcripts and two were

Table 1 Transcripts of putative chemosensory genes upregulated in mite’s body with both the gnathosoma and forelegs (WB_plus), mites without both the gnathosoma and forelegs (WB_minus), gnathosoma or forelegs. The data are the total number of transcripts detected or upregulated in each group

Chemosensory group	Total number of chemosensory transcripts detected and upregulated				
	Detected in whole body	Upregulated in WB_plus	Upregulated in WB_minus	Upregulated in gnathosoma	Upregulated in forelegs
Soluble carrier proteins					
Insect OBPs	5	–	1	2	1
OBP-like	2	1	1	1	1
NPC2	4	1	–	–	1
lipocalins	6	1	2	–	3
Receptors and membrane bound proteins					
IGRs	25	2	1	2	–
IRs	1	–	–	–	1
GRs	2	–	–	1	1
SNMPs	5	–	1	–	–
TRPs	21	–	3	2	–
ENaCs	12	–	1	–	3

–No transcript was upregulated

OBP-like transcripts), four to the NPC2 families, and six to the Lipocalin family. Among the membrane-bound proteins, we identified 26 ionotropic receptors (25 of the IGR family and one from the IR subfamily), two GR proteins, five SNMPs, 21 TRPs and 12 ENaCs transcripts (Table 1). We further checked if these transcripts are also translated into proteins in the *Varroa* gnathosoma. The *Varroa* gnathosoma proteome yielded a total of 2,795 proteins, of which 1,758 were supported by more than one peptide (Supplementary Table S3). Of the chemosensory transcripts, eight out of the 17 lipid carrier proteins were also identified in the proteome, and 13 out of the 66 membrane-bound proteins had a corresponding protein (Fig. 2).

Silencing of target LOC111245174 transcript

The survival rates after 15 h of soaking in saline or Vd105872-dsRNA solutions 2.5 µg/µl and 4 µg/µl solution of dsRNA and a control template were: 77% vs. 65%, 63% and 69% respectively. However, the GR gene transcript (LOC111245174) was not silenced in mites soaked in either 2.0, 2.5–4 µg/µl dsRNA solution when compared to non-silenced control mites (One-way Anova: $F_{(2,16)}=0.16$, $p=0.85$, Supplementary Fig. S2).

Discussion

Through transcriptomic and proteomic analyses, our results revealed that *Varroa*'s gnathosoma expresses proteins from the same groups of putative chemosensory transcripts that were previously reported in the forelegs (Eliash et al. 2019) including lipocalin (Fig. 2). This suggests the existence of two functional chemosensory systems in *Varroa* that share some common molecular features. Yet, both organs differ in the expression profiles of some putative lipid carrier proteins (OBP-like, NPC2 and lipocalins), membrane-bound receptors and associated proteins (IGRs, IR, TRPs and ENaCs) (Fig. 2). This further suggests that the two organs may not necessarily perform the same sensory functions since we previously demonstrated that the gnathosoma sensilla have a minor chemosensory function in terms of host recognition when compared to those of the forelegs (Nganso et al. 2020).

The lack of the CSP lipid carrier and the OR groups in the whole body of the mite strongly supports previous studies that reported the absence of these chemosensory groups in *Varroa* (Eliash et al. 2017, 2019; Iovinella et al. 2018). Although the CSP group has been reported in the genomes of all arthropods (Gulia-Nuss et al. 2016; Eyun et al. 2017), including two chelicerate species: the Baja California bark scorpion, *Centruroides exilicauda*, and the western black widow spider, *Lactrodectus hesperus* (Eyun et al. 2017) and one Acari, *Ixodes scapularis* (Gulia-Nuss et al. 2016; Eyun et al. 2017), their function in Acari remains inconclusive. Further, our findings confirm once again the complete absence of OR genes in Chelicerata examined to date (Brand et al. 2018; Eyun et al. 2017; Vizueta et al. 2018). Taken together, our results suggest that the molecular features of these chemosensory organs resemble mostly those of their close chelicerate relatives and in some ways those of their distantly related Crustacea and Myriapoda relatives, as demonstrated before (Vizueta et al. 2018).

Chemosensory transcripts are expressed in all body parts

In this study, it was interesting to note that all 83 chemosensory transcripts are also expressed in the whole body and the whole body devoid of the two chemosensory appendages (Fig. 2). In particular, seven of these 83 transcripts were highly expressed in the whole body devoid of the two chemosensory appendages compared to the gnathosoma (Fig. 2). They include one insect OBP (LOC111243821) and OBP-like (LOC111247024), two lipocalins (LOC111249022, LOC111250379), one TRP (LOC111251668, LOC111243271) and ENaC (LOC111253877) transcripts. Indeed, it has been reported that some of these chemosensory genes such as OBPs and NPC2s (Pelosi et al. 2014, 2018; Bhowmick et al. 2020), lipocalins (Zhu et al. 2021a), GRs and IRs (Ngoc et al. 2016; Vizueta et al. 2018), TRPs (Kozma et al. 2018), ENaCs (Ben-Shahar 2011; Ngoc et al. 2016) are also expressed in other parts of the body. This suggests that chemosensory functions of these transcripts are likely to extend to other body parts or their functions may extend beyond chemoreception of the external cues in some arthropod groups including mites and ticks, similar to findings in vertebrates (Berg and Kaunitz 2016). Future annotation studies via techniques such as RNA interference (RNAi) or the bacterial type II Clustered Regularly Interspaced Short Palindromic Repeats and associated protein 9 (CRISPR-Cas9) system (Nganso et al. 2022) will be needed to enhance our understanding of the role of these transcripts in mite's body function.

Soluble carrier proteins function in both short- and long-range chemoreception

Of the seven OBP transcripts found in this study, six were originally reported in *Varroa*'s forelegs (Fig. 2). The new OBP transcript detected in this study (LOC111255133), was classified as an insect OBP-related transcript because it contains both the conserved insect-OBP domain (IPR036728) and the GO-term of "odorant binding" (GO-0005549). It is worth mentioning that our previous exclusion assay's study demonstrated that two OBP transcripts previously reported in *Varroa* (Eliash et al. 2019) were foreleg-specific as their expression levels dropped significantly following the removal of the forelegs (Nganso et al. 2021). In this study, we detected only one out of these two transcripts (LOC111247116) in gnathosoma, but neither of the corresponding protein products were found in the gnathosoma proteome of this study or in the foreleg proteome from previous studies (Eliash et al. 2019's study). This might indicate a short lifespan or low abundance of the protein product of this transcript (Nganso et al. 2022). Moreover, the sensitivity of the methods used in the previous and this study could also explain the lack of detection of the protein product of this transcript.

Interestingly, a specific NPC2 transcript (LOC111247660) was significantly upregulated in the forelegs when compared to the rear legs and the gnathosoma relative to the whole body without chemosensory organs (Fig. 2). This result confirmed our previous exclusion study that demonstrated that the expression level of this transcript dropped significantly in the absence of the forelegs (Nganso et al. 2021). Knockdown of this highly expressed and foreleg-specific transcript via RNA interference suggests that it might be involved in the detection of short-range cues because *Varroa*'s feeding and reproduction were significantly reduced following its silencing (Nganso et al. 2021). Similarly, a second NPC2 transcript (LOC111247342), whose expression was shown to be similar in both the foreleg and the gnathosoma via the exclusion assay (Nganso et al. 2021), appears to be expressed at low levels

in both chemosensory appendages (Fig. 2). Contrary to the first annotated NPC2 transcript, silencing this transcript affected *Varroa*-host reaching ability suggesting its involvement in the detection of long-range cues (Mani et al. 2022). Given these results, it seems that both appendages are equipped with lipid binding proteins enabling them to solubilize different odorant molecules and carry the latter to the chemoreceptors in the chemosensory sensilla.

Six out of the nine lipocalins reported in the genome of *Varroa* mite (Zhu et al. 2021a) were found in this study (Fig. 2). Of the six sequences of lipocalins detected, it was interesting to note that three (LOC111247224, LOC111251803 and LOC111251576) were highly expressed in the mite forelegs compared to the rear legs, and none in the gnathosoma. The fact that the corresponding protein products of none of these upregulated lipocalin transcripts were not detected in the gnathosoma's proteome may be due to the factors highlighted above and may suggest that the CRISPR-Cas9 system might be used in future for their functional annotation (Nganso et al. 2022). Overall, our results indicate that in the absence of CSP, these lipocalin transcripts could represent another group of semiochemical carriers in *Varroa* in particular as well as in other chelicerates, crustaceans and hexapods in which they were found to be highly expressed in chemosensory structures earlier by Zhu et al. (2021a).

Taste and olfactory chemoreceptor's potential role in short range chemoperception

As opposed to the somewhat general expression of the soluble carrier proteins, transcripts of the membrane-bound receptors of the IGR and GR families were upregulated in the gnathosoma more than in any other body parts (Fig. 2). Proteins of these groups are known to be involved in olfaction (smell) and gustation (taste) in chelicerates in the absence of OR group (Vizueta et al. 2018; Su et al. 2021). The gnathosoma-specific expression of these transcripts could be adaptive as the mite primarily uses its gnathosoma to sense and taste its suitable host stage to ensure its feeding and reproduction, whereas the forelegs are primarily raised above the surface in a similar manner to the antennae of other arthropods for volatile detection. In fact, the two IGR transcripts (LOC111247324 and LOC111248674) were significantly (or close to significant) upregulated in the gnathosoma, while none were upregulated in the foreleg (Fig. 2). Both of these upregulated transcripts contained the two essential characteristic domains of the IGR superfamily (IPR019594 and IPR001320) and were also present in the proteome of the gnathosoma, suggesting that their proteins are abundant. Moreover, one GR transcript (LOC111245174, referred to as *Vd105872* in Eliash et al. 2017) was significantly upregulated in the gnathosoma and the forelegs, suggesting that it is probably involved in both gustation and olfaction. The fact that it was not found in the proteome of neither gnathosoma (this study) nor in the foreleg in Eliash et al. 2019 may as in previous cases suggest low abundance and/or short life of its protein. Intriguingly, our attempts to silence the expression of this gene by RNAi failed and could be due to the factors mentioned above. Further, not all genes can be silenced by RNAi as gene silencing is a “tricky” operation and may be impacted by the interaction between the siRNA and the other RNAi pathways (Ghildiyal and Zamore 2009; Yang et al. 2020; Nganso et al. 2022). Perhaps, functional analyses using other approaches such as CRISPR-Cas9 (the bacterial type II Clustered Regularly Interspaced Short Palindromic Repeats and associated protein 9 system) and/or the *Xenopus* oocyte expression system could elucidate the function of this gene in *Varroa*-honey bee chemosensing. The other GR (GR2) transcript (LOC111254617,

referred to as *Vd7144* in Eliash et al. 2017) was not upregulated in the foreleg or gnathosoma, and its product was absent from the proteome of the gnathosoma and in the former foreleg's proteome (Eliash et al. 2019). It is worth indicating that this GR2 transcript is apparently an isoform of an additional GR transcript found previously in *Varroa*' forelegs (Eliash et al. 2017, 2019; former name Trinity_DN29661_c0_g1) and named there as GR3. In *Varroa* forelegs, only one potential IR transcript (LOC111251297, referred to as *Vd17150* in Eliash et al. 2017), which is an IR25a-like homologue and contains the two essential characteristic domains of the IGR superfamily was significantly upregulated (Fig. 2). But the product of this transcript was not found in the proteome of the gnathosoma (in this study) and that of the foreleg (Eliash et al. 2019). We also found that this IR25a transcript is an isoform of an additional IR (IR1) transcript (referred to as Trinity_DN26056_c0_g1_i2 and *Vd19098* in Eliash et al. 2019 and 2017; respectively) found previously in *Varroa* forelegs (Eliash et al. 2017, 2019). Recently, we showed that the IR25a (LOC111251297) and GR1 (LOC111245174) transcripts are co-expressed with transcripts of some lipid carrier proteins in the putative gene networks we built, further supporting their role in *Varroa*'s chemoreception (Mani et al. 2022).

Among the SNMP chemosensory associated proteins, which contain the conserved domain of the CD36 receptor family, our study did not reveal any significantly upregulated transcripts in either the foreleg or gnathosoma (Fig. 2). This suggests that this group is unlikely to play a role in chemosensation in *Varroa*. It is worth mentioning that members of the CD36-SNMP group have been reported in other arthropods including hexapods, myriapods and crustaceans studied to date (Vizueta et al. 2018; Su et al. 2021), and recently their role in sex pheromone detection in *Bombyx mori* was demonstrated (Zhang et al. 2018). Regarding the specialized ion channel receptor families of TRP and ENaC, two TRP transcripts (LOC111243805, LOC111248665) were significantly upregulated in the gnathosoma but no ENaC transcripts were upregulated in this organ (Fig. 2). On the other hand, in the mite's forelegs, none of the potential TRPs were upregulated while three ENaCs (LOC111254848, LOC111244963 and LOC111251329) were significantly upregulated. This suggests that transcripts of TRP and ENaCs, which are upregulated in the chemosensory appendages, could play a role in *Varroa*-honey bee interaction. Co-expression networks presented in previous study also pointed towards the involvement of TRP1 in this process (Mani et al. 2022). Orthologs of ENaCs and TRPs were reported in other arthropods including mites and ticks (Ngoc et al. 2016; Kozma et al. 2020), but their role in chemoreception has not yet been extensively elucidated. However, the role of TRP in reception of plant-derived volatiles was recently demonstrated both in Chelicerates, specifically in *V. destructor* (Peng et al. 2015), and insects (Tian et al. 2022). The latter manuscripts further suggested this receptor as a potential target in development of new methods for Arthropod pest management.

In conclusion, comparative transcriptomic and proteomic analyses revealed the presence of the putative chemosensory related transcripts belonging to several groups based on conserved domain search in the whole body, gnathosoma, and body devoid of the two chemosensory organs of the honey bee parasitic *Varroa* mite. To the best of our knowledge, this is the first study that compares the expression of transcripts from several chemosensory-related groups between these body parts of a mite. Through this study, we confirm that *Varroa*'s gnathosoma possesses chemosensory abilities given the expression of families of chemosensory genes that were previously reported in the mite's forelegs (Eliash et al. 2017,

2019) as well as additional ones. The exact site of chemosensory organs in gnathosoma is still not clear, though some sensilla on the mite's palpi were found before (Liu and Peng 1990). Given the differences in the expression profiles of some putative chemosensory genes between the forelegs and the gnathosoma, our results suggest that these two chemosensory systems apparently differ in characteristics of compounds that are detected. These differences in detection abilities will require further studies, as well as the function of the putative chemosensory transcripts found in the body deprived forelegs and gnathosoma. Could there be additional chemosensory organs not yet revealed? On the other hand, could these transcripts have other roles such as in internal body communication? Our results emphasize the complexity of detection and annotation of chemosensory-related proteins that involves the combination of both behavioral and molecular approaches. Ideally, the combination of the molecular manipulations such as gene-knockdown (RNAi) or CRISPR-cas9, in addition to the recently improved tool of protein fold prediction (Jumper et al. 2021), will help to confirm the role of suspected proteins, and more importantly, the detection of new ones.

Supplementary Information The online version contains supplementary material available at <https://doi.org/10.1007/s10493-024-00952-1>.

Acknowledgements We wish to thank Mr. Yosef Kamer and Mr. Assaf Otmy for their dedicated care of the honey bee colonies. This research was funded by the Israel Science Foundation to Victoria Soroker and Ada Rafaeli (No. 1973/18), and the Japan Society for the Promotion of Science - and the Israel Science Foundation joint fund (No. 120208404) to Victoria Soroker and Alexander Mikheyev. The funding agencies had no role in the study design, data collection and analysis, decision to publish, or preparation of the manuscript.

Author contributions Conceived and designed the study, V.S. and A.R.; collected the data, B.T.N., K.M. and F.O.; analyzed the data, N.S., N.E., A.V-B., V.S.; writing – original draft preparation, B.T.N. and V.S.; writing – review and editing, V.S., A.R., A.S.M., B.T.N., N.E. The author(s) read and approved the final manuscript.

Funding This research was supported by Israel Science Foundation Grant to V.S. and A.R. (No. 1973/18). Open access funding provided by The Agricultural Research Organization of Israel.

Data availability The raw read sequences from the three RNA samples from *Varroa* mite were uploaded to the National Centre for Biotechnology Information (NCBI) on accession No^o PRJNA872955. Proteomic data are available via ProteomeXchange with identifier PXD053065.

Declarations

Ethical approval Not applicable.

Consent to participate Not applicable.

Consent for publication Not applicable.

Conflict of interest The authors declare no conflict of interest.

Open Access This article is licensed under a Creative Commons Attribution 4.0 International License, which permits use, sharing, adaptation, distribution and reproduction in any medium or format, as long as you give appropriate credit to the original author(s) and the source, provide a link to the Creative Commons licence, and indicate if changes were made. The images or other third party material in this article are included in the article's Creative Commons licence, unless indicated otherwise in a credit line to the material. If material is not included in the article's Creative Commons licence and your intended use is not permitted by statutory regulation or exceeds the permitted use, you will need to obtain permission directly from the copyright holder. To view a copy of this licence, visit <http://creativecommons.org/licenses/by/4.0/>.

References

- Aird SD, Watanabe Y, Villar-Briones A, Roy MC, Terada K, Mikheyev AS (2013) Quantitative high-throughput profiling of snake venom gland transcriptomes and proteomes (*Ovophis okinavensis* and *Protobothrops flavoviridis*). *BMC Genom* 14:1–27. <https://doi.org/10.1186/1471-2164-14-790>
- Anders S, Huber W, Nagalakshmi U, Wang Z, Waern K, Shou C, Raha D, Gerstein M, Snyder M, Mortazavi A, Williams BA, McCue K, Schaeffer L, Wold B, Robertson G, Hirst M, Bainbridge M, Bilenky M, Zhao Y, Zeng T, Euskirchen G et al (2010) Differential expression analysis for sequence count data. *Genome Biol* 11:R106. <https://doi.org/10.1186/gb-2010-11-10-r106>
- Ben-Shahar Y (2011) Sensory functions for degenerin/epithelial sodium channels (DEG/ENaC). *Adv Genet* 76:1–26. <https://doi.org/10.1016/B978-0-12-386481-9.00001-8>
- Benjamini Y, Hochberg Y (1995) Controlling the false discovery rate: a practical and powerful approach to multiple testing. *J R Stat Soc B* 57:289–300. <https://doi.org/10.1111/j.2517-6161.1995.tb02031.x>
- Berg CJ, Kaunitz JD (2016) Gut chemosensing: implications for disease pathogenesis. *F1000Res* 5:2424. <https://doi.org/10.12688/f1000research.9208.1>
- Bhowmick B, Tang Y, Lin F, Øines Ø, Zhao J, Liao C, Ignell R, Hansson BS, Han Q (2020) Comparative morphological and transcriptomic analyses reveal chemosensory genes in the poultry red mite, *Dermanyssus gallinae*. *Sci Rep* 10:17923–17938. <https://doi.org/10.1038/s41598-020-74998-7>
- Bolger AM, Lohse M, Usadel B (2014) Trimmomatic: a flexible trimmer for Illumina sequence data. *Bioinformatics* 30:2114–2120. <https://doi.org/10.1093/bioinformatics/btu170>
- Brand P, Robertson HM, Lin W, Pothula R, Klingeman WE, Jurat-Fuentes JL, Johnson BR (2018) The origin of the odorant receptor gene family in insects. *Elife* 7:e38340. <https://doi.org/10.7554/eLife.38340>
- Dietemann V, Nazzi F, Martin SJ, Anderson DL, Locke B, Delaplane KS, Wauquiez Q, Tannahill C, Frey E, Ziegelmann B, Rosenkranz P, Ellis JD (2013) Standard methods for *Varroa* research. *J Apic Res* 52:1–54. <https://doi.org/10.3896/IBRA.1.52.1.09>
- Dillier F-X, Fluri P, Imdorf A (2006) Review of the orientation behaviour in the bee parasitic mite *Varroa destructor*. <https://doi.org/10.5962/bhl.part.80381>
- Eliash N, Singh NK, Kamer Y, Pinnelli GR, Plettner E, Soroker V (2014) Can we disrupt the sensing of honey bees by the bee parasite *Varroa destructor*? *PLoS ONE* 9:e106889. <https://doi.org/10.1371/journal.pone.0106889>
- Eliash N, Singh NK, Thangarajan S, Sela N, Leshkowitz D, Kamer Y, Zaidman I, Rafaeli A, Soroker V (2017) Chemosensing of honeybee parasite, *Varroa destructor*: transcriptomic analysis. *Sci Rep* 7(1):13091. <https://doi.org/10.1038/s41598-017-13167-9>
- Eliash N, Thangarajan S, Goldenberg I, Sela N, Kupervaser M, Barlev J, Altman Y, Knyazer A, Kamer Y, Zaidman I, Rafaeli A, Soroker V (2019) *Varroa* chemosensory proteins: some are conserved across Arthropoda but others are arachnid specific. *Insect Mol Biol* 28:321–341. <https://doi.org/10.1111/imb.12553>
- Eyun SI, Soh HY, Posavi M, Munro JB, Hughes DS, Murali SC, Qu J, Dugan S, Lee SL, Chao H, Dinh H (2017) Evolutionary history of chemosensory-related gene families across the Arthropoda. *Mol Biol Evol* 34:1838–1862. <https://doi.org/10.1093/molbev/msx147>
- Frey E, Odemer R, Blum T, Rosenkranz P (2013) Activation and interruption of the reproduction of *Varroa destructor* is triggered by host signals (*Apis mellifera*). *J Invertebr Pathol* 113:56–62. <https://doi.org/10.1016/j.jip.2013.01.007>
- Ghildiyal M, Zamore PD (2009) Small silencing RNAs: an expanding universe. *Nat Rev Genet* 10(2):94–108. <https://doi.org/10.1038/nrg2504>
- Gulia-Nuss M, Nuss AB, Meyer JM, Sonenshine DE, Roe RM, Waterhouse RM, Sattelle DB, De La Fuente J, Ribeiro JM, Megy K, Thimmapuram J (2016) Genomic insights into the *Ixodes scapularis* tick vector of Lyme disease. *Nat Commun* 7:1–13. <https://doi.org/10.1038/ncomms10507>
- Haas BJ (n.d.) TransDecoder [WWW Document (ed)]. TransDecoder. URL <https://github.com/TransDecoder/TransDecoder> (accessed 19)
- HaileMariam M, Eguez RV, Singh H, Bekele S, Ameni G, Pieper R, Yu Y (2018) S-Trap, an ultrafast sample-preparation approach for shotgun proteomics. *J Proteome Res* 17:2917–2924. <https://doi.org/10.1021/acs.jproteome.8b00505>
- Iovinella I, McAfee A, Mastrobuoni G, Kempa S, Foster LJ, Pelosi P, Dani FR (2018) Proteomic analysis of chemosensory organs in the honey bee parasite *Varroa destructor*: a comprehensive examination of the potential carriers for semiochemicals. *J Proteom* 181:131–141. <https://doi.org/10.1016/j.jprot.2018.04.009>

- Jumper J, Evans R, Pritzel A, Green T, Figurnov M, Ronneberger O, Tunyasuvunakool K, Bates R, Židek A, Potapenko A, Bridgland A, Meyer C, Kohl SAA, Ballard AJ, Cowie A, Romera-Paredes B, Nikolov S, Jain R, Adler J, Back T, Petersen S, Reiman D, Clancy E, Zielinski M, Steinegger M, Pacholska M, Berghammer T, Bodenstein S, Silver D, Vinyals O, Senior AW, Kavukcuoglu K, Kohli P, Hassabis D (2021) Highly accurate protein structure prediction with alpha fold. *Nature* 596:583–589. <https://doi.org/10.1038/s41586-021-03819-2>
- Kim D, Perteua G, Trapnell C, Pimentel H, Kelley R, Salzberg SL (2013) TopHat2: accurate alignment of transcriptomes in the presence of insertions, deletions and gene fusions. *Genome Biol* 14:1–3. <https://doi.org/10.1186/gb-2013-14-4-r36>
- Kozma MT, Schmidt M, Ngo-Vu H, Sparks SD, Senatore A, Derby CD (2018) Chemoreceptor proteins in the Caribbean spiny lobster, *Panulirus argus*: expression of ionotropic receptors, gustatory receptors, and TRP channels in two chemosensory organs and brain. *PLoS ONE* 13:e0203935. <https://doi.org/10.1371/journal.pone.0203935>
- Kozma MT, Ngo-Vu H, Wong YY, Shukla NS, Pawar SD, Senatore A, Schmidt M, Derby CD (2020) Comparison of transcriptomes from two chemosensory organs in four decapod crustaceans reveals hundreds of candidate chemoreceptor proteins. *PLoS ONE* 15:e0230266. <https://doi.org/10.1371/journal.pone.0230266>
- Liu TP, Peng Y-S (1990) Palpal tarsal sensilla of the female mite, *Varroa jacobsoni* Oud. *Can Entomol* 122:295–300. <https://doi.org/10.4039/Ent122295-3>
- Mani K, Nganso BT, Rodin P, Otmay A, Rafaeeli A, Soroker V (2022) Effects of Niemann-pick type C2 (NPC2) gene transcripts silencing on behavior of *Varroa destructor* and molecular changes in the putative olfactory gene networks. *Insect Biochem Mol Biol* 148:103817. <https://doi.org/10.1016/j.ibmb.2022.103817>
- Martin SJ (2001) Biology and life history of *Varroa* mites, in: Webster, T.C., Delaplane, K.S. (Eds.), *Mites of the honey bee*. Dadant, Sons, Hamilton, pp. 131–148. https://doi.org/10.1007/978-1-4020-6359-6_3938
- Nazzi F, Le Conte Y (2016) Ecology of *Varroa destructor*, the major ecto-parasite of the western honey bee, *Apis mellifera*. *Annu Rev Entomol* 61:417–432. <https://doi.org/10.1146/annurev-ento-010715-023731>
- Nganso BT, Mani K, Altman Y, Rafaeeli A, Soroker V (2020) How crucial is the functional pit organ for the *Varroa* Mite? *Insects* 11:395–406. <https://doi.org/10.3390/insects11060395>
- Nganso BT, Mani K, Eliash N, Rafaeeli A, Soroker V (2021) Towards disrupting *Varroa*-Honey bee chemosensing: a focus on a Niemann-pick type C2 transcript. *Insect Mol Biol* 30:519–531. <https://doi.org/10.1111/imb.12722>
- Nganso BT, Pines G, Soroker V (2022) Insights into gene manipulation techniques for Acari functional genomics. *Insect Biochem Mol Biol* 143:103705–103714.
- Ngoc PCT, Greenhalgh R, Dermauw W, Rombauts S, Bajda S, Zhurov V, Grbić M, Van de Peer Y, Van Leeuwen T, Rouze P, Clark RM (2016) Complex evolutionary dynamics of massively expanded chemosensory receptor families in an extreme generalist chelicerate herbivore. *Genome Biol Evol* 8:3323–3339. <https://doi.org/10.1093/gbe/evw249>
- Oliveros JC (2007–2015) Venny. An interactive tool for comparing lists with Venn's diagrams [WWW Document]. URL <https://bioinfogp.cnb.csic.es/tools/venny/index.html>
- Pelosi P, Iovinella I, Felicioli A, Dani FR (2014) Soluble proteins of chemical communication: an overview across arthropods. *Front Physiol* 5:320–333. <https://doi.org/10.3389/fphys.2014.00320>
- Pelosi P, Iovinella I, Zhu J, Wang G, & Dani FR (2018) Beyond chemoreception: diverse tasks of soluble olfactory proteins in insects. *Biological Reviews*, 93(1), 184–200. <https://doi.org/10.1111/brv.12339>
- Peng G, Kashio M, Morimoto T, Li T, Zhu J, Tominaga M, Kadowaki T (2015) Plant-derived tick repellents activate the honey bee ectoparasitic mite TRPA1. *Cell Reports* 12(2):190–202. <https://doi.org/10.1016/j.celrep.2015.06.025>
- Perez-Riverol Y, Bai J, Bandla C, Garcia-Seisdedos D, Hewapathirana S, Kamatchinathan S, Kundu DJ, Prakash A, Frericks-Zipper A, Eisenacher M, Walzer M, Wang S, Brazma A, Vizcaino JA (2022) The PRIDE database resources in 2022: a hub for mass spectrometry-based proteomics evidences. *Nucleic Acids Res* 50:D543–D552
- Pernal SF, Baird DS, Birmingham AL, Higo HA, Slessor KN, Winston ML (2005) Semiochemicals influencing the host-finding behaviour of *Varroa destructor*. *Exp Appl Acarol* 37:1–26. <https://doi.org/10.1007/s10493-005-1117-x>
- Plettner E, Eliash N, Singh NK, Pinnelli GR, Soroker V (2017) The chemical ecology of host-parasite interaction as a target of *Varroa destructor* control agents. *Apidologie* 48:1–15. <https://doi.org/10.1007/s13592-016-0452-8>
- Quevillon E, Silventoinen V, Pillai S, Harte N, Mulder N, Apweiler R, Lopez R (2005) InterProScan: protein domains identifier. *Nucleic Acids Res* 33:W116–W120. <https://doi.org/10.1093/nar/gki442>
- Rappsilber J, Mann M, Ishihama Y (2007) Protocol for micro-purification, enrichment, pre-fractionation and storage of peptides for proteomics using StageTips. *Nat Protoc* 8:1896–1906. <https://doi.org/10.1038/nprot.2007.261>

- Rosenkranz P, Aumeier PIA, Ziegelmann B (2010) Biology and control of *Varroa destructor*. *J Invertebr Pathol* 103:96–119. <https://doi.org/10.1016/j.jip.2009.07.016>
- Singh NK, Nurit E, Pinnelli GR, Kamer Y, Zaidman I, Plettner E, Soroker V (2015) Specific disruption of *Varroa* chemosensing. In *Congreso Int De Actualización Apícola* 73–77
- Soroker V, Singh NK, Eliash N, Plettner E (2019) Olfaction as a target for control of honeybee parasite mite *Varroa destructor*, in: *Olfactory concepts of pest control—Alternative to insecticides*. J-F. Picimbon ed. Springer. Cham. Pp.117–134. https://doi.org/10.1007/978-3-030-05060-3_6
- Su Y, Zhang B, Xu X (2021) Chemosensory systems in predatory mites: from ecology to genome. *Syst Appl Acarol* 26:852–865. <https://doi.org/10.11158/saa.26.5.3>
- Techer MA, Rane RV, Grau ML, Roberts JMK, Sullivan ST, Liachko I, Childers AK, Evans JD, Mikheyev AS (2019) Divergent evolutionary trajectories following speciation in two ectoparasitic honey bee mites. *Commun Biol* 2:357–373. <https://doi.org/10.1038/s42003-019-0606-0>
- Tian Q, Wang P, Xie C, Pang P, Zhang Y, Gao Y, Cao Z, Wu Y, Li W, Zhu MX, Li D (2022) Identification of an arthropod molecular target for plant-derived natural repellents. *Proc Natl Acad Sci* 119(18):e2118152119. <https://doi.org/10.1073/pnas.2118152119>
- Trapnell C, Roberts A, Goff L, Pertea G, Kim D, Kelley DR, Pimentel H, Salzberg SL, Rinn JL, Pachter L (2012) Differential gene and transcript expression analysis of RNA-seq experiments with TopHat and cufflinks. *Nat Protoc* 7:562–578. <https://doi.org/10.1038/nprot.2012.016>
- Traynor KS, Mondet F, de Miranda JR, Techer M, Kowallik V, Oddie MAY, Chantawannakul P, McAfee A (2020) *Varroa destructor*: a complex parasite, crippling honey bees worldwide. *Trends Parasitol* 36:592–606. <https://doi.org/10.1016/j.pt.2020.04.004>
- Vizueta J, Rozas J, Sánchez-Gracia A (2018) Comparative genomics reveals thousands of novel chemosensory genes and massive changes in chemoreceptor repertoires across chelicerates. *Genome Biol Evol* 10(5):1221–1236. <https://doi.org/10.1093/gbe/evy081>
- Yang L, Tian Y, Peng YY, Niu J, Wang JJ (2020) Expression dynamics of core RNAi machinery genes in pea aphids upon exposure to artificially synthesized dsRNA and miRNAs. *Insects* 11(2): 70–84. <https://doi.org/10.3390/insects11020070>
- Zhang HJ, Xu W, Chen QM, Sun LN, Anderson A, Xia QY, Papanicolaou A (2018) Functional characterization of sensory neuron membrane proteins (SNMPs). *BioRxiv* 262154–262181
- Zhu J, Iannucci A, Dani FR, Knoll W, Pelosi P (2021a) Lipocalins in Arthropod Chemical Communication. *Genome Biol Evol* 13:evab091. <https://doi.org/10.1093/gbe/evab091>
- Zhu J, Renzone G, Arena S, Dani FR, Paulsen H, Knoll W, Cambillau C, Scaloni A, Pelosi P (2021b) The odorant-binding proteins of the spider mite *tetranychus urticae*. *Int J Mol Sci* 22:6828–6849. <https://doi.org/10.3390/ijms22136828>

Publisher's Note Springer Nature remains neutral with regard to jurisdictional claims in published maps and institutional affiliations.

Authors and Affiliations

Beatrice T. Nganso^{1,2} · Nurit Eliash^{3,4,5} · Kannan Mani¹ · Noa Sela⁶ · Alejandro Villar-Briones⁷ · Angelina Fathia Osabutey¹ · Ada Rafaeli⁸ · Alexander S. Mikheyev^{3,9} · Victoria Soroker¹

✉ Victoria Soroker
sorokerv@volcani.agri.gov.il

¹ Department of Entomology, Institute of Plant Protection, Agricultural Research Organization, the Volcani Center, Rishon LeZion, Israel

² International Centre of Insect Physiology and Ecology (icipe), Nairobi, Kenya

³ Ecology and Evolution Unit, Okinawa Institute of Science and Technology Onna-son, Okinawa, Japan

⁴ Shamir Research Institute, Rishon LeTsiyon, Israel

⁵ University of Haifa, Haifa, Israel

⁶ Bioinformatics Unit, ARO Volcani Center, 68 HaMaccabim Road, P.O.B 15159, Rishon LeZion 7528809, Israel

⁷ Instrumental Analysis Section, Okinawa Institute of Science and Technology Graduate University, Okinawa, Japan

⁸ Institute of Postharvest and Food Sciences, Agricultural Research Organization, the Volcani Centre, Rishon Lezion, Israel

⁹ Research School of Biology, Australian National University, Canberra, ACTRR, Australia